

Article

## Selective Production of Aromatics from 2-Octanol on Zinc Ion-Exchanged MFI Zeolite Catalysts

Masakazu Iwamoto <sup>1,\*</sup>, Ryota Takezawa <sup>2,†</sup> and Masao Morimoto <sup>2,†</sup>

<sup>1</sup> Research and Development Initiative, Chuo University, 1-13-27 Kasuga, Bunkyo-ku, Tokyo 112-8551, Japan

<sup>2</sup> Technology Development Division, Toray Fine Chemicals Co., Ltd., 2-3 Chigusakaigan, Ichihara, Chiba 299-0196, Japan; E-Mails: ryota\_takezawa@tfc.toray.co.jp (R.T.); masao\_morimoto@tfc.toray.co.jp (M.M.)

† These authors contributed equally to this work.

\* Author to whom correspondence should be addressed; E-Mail: iwamotom@tamacc.chuo-u.ac.jp; Tel./Fax: +81-3-3817-1612.

Academic Editor: Rafael Luque

Received: 13 November 2015 / Accepted: 30 November 2015 / Published: 10 December 2015

---

**Abstract:** The aromatization of 2-octanol derived from castor oil as a byproduct in the formation of sebacic acid was investigated on various zeolite catalysts. Zn ion-exchanged MFI (ZSM-5) zeolites with small silica/alumina ratios and zinc contents of 0.5 to 2.0 wt. % were determined to exhibit good and stable activity for the reaction at 623 to 823 K. The yield of aromatics was 62% at 773 K and the space velocity 350 to 1400 h<sup>-1</sup>. The temperature and contact time dependences of the product distributions indicated the reaction pathways of 2-octanol→dehydration to 2-octene→decomposition to C<sub>5</sub> and C<sub>3</sub> compounds→further decomposition to small alkanes and alkenes→aromatization with dehydrogenation. Alcohols with carbon numbers of 5 to 8 exhibited similar distributions of products compared to 2-octanol, while corresponding carbonyl compounds demonstrated different reactivity.

**Keywords:** 2-octanol; aromatization; MFI zeolites; zinc ion; biomass

---

## 1. Introduction

Approximately 1.3 million tons of castor oil is produced annually worldwide and is used as a typical biomass material [1]. Recently, castor oil's application has been expanded to the manufacturing of 6,10-nylon. In the polymer synthesis industry, ricinoleic acid (a compound consisting of 18 carbon atoms, C<sub>18</sub>) was first produced by the transesterification of castor oil with methanol, and subsequently decomposed to sebacic acid (C<sub>10</sub>) and 2-octanol (C<sub>8</sub>). Sebacic acid yields 6,10-nylon via the reaction with hexamethylenediamine [2]. However, the remaining 2-octanol is partially used as, for instance, a lubricant and plasticizer [3], but its usage is limited, and new applications should be developed. Moreover, the use of shale gas for energies and chemicals has rapidly grown worldwide, which changes the construction of the current petroleum chemistry [4–6]. The lack of aromatics, the production of which from shale gas is notably difficult, has been a severe challenge which should be resolved in the shale gas industry. We proposed that the selective conversion of 2-octanol to aromatics would be significant to generate a new type of environmentally benign chemistry to cope with the shale gas industry. This developed method would be able to be expanded into other biomass products. This possibility was investigated in this study and good results were obtained.

The aromatization of various compounds, including alcohols [5–12], alkanes [13–21], and alkenes [22], has been reported on various heterogeneous catalysts, such as silica-alumina, zeolites, hydroxyapatite, and heteropolyacids. Our attention was focused on zeolite catalysts based on the following reports. The selectivity of aromatics on zeolite catalysts was the highest among those on reported catalysts due to the shape selectivity [13–21]. Platinum-loaded K-LTL zeolites were reported as highly active catalysts for the aromatization of *n*-hexane [23–28]. In addition, proton and metal ion-exchanged MFI zeolites exhibited high activity for the formation of gasoline from various alcohols [7]. The reactivity of 2-octanol on various zeolites was first investigated here. The effects of the silica/alumina ratio and the loaded metal ion on the catalytic activity were subsequently examined. The product distributions were investigated as a function of the amount of active metal ions and the gas hourly space velocity (GHSV). Finally, the reaction pathways were discussed based on the temperature and the contact time dependences of the product distribution and the reactivity of other reactants.

It should be noted that the industrial production of 2-octanol is accompanied with a by-product, methyl *n*-hexyl ketone (2-octanone). Hence, technical 2-octanol as prepared by the present industrial process is a mixture of about 85% 2-octanol and 15% 2-octanone by weight. The reactivity of 2-octanone was also measured in this study to reveal the effect of the impurity for the aromatization of 2-octanol.

## 2. Results and Discussion

### 2.1. Carbon Balance of the Reaction and Stability of the Catalyst

Before the detailed introduction of the experimental results, the carbon balance of the reaction and the stability of the typical catalyst developed in the current study are summarized in Figure 1. The catalyst employed here was a Zn-MFI catalyst with Zn of 0.25 wt. %, which was prepared using H-MFI with a silica/alumina ratio of 40. As described in the experimental section, we determined either the amounts of C<sub>5</sub>–C<sub>8</sub> compounds or C<sub>3</sub>–C<sub>4</sub> compounds in one experiment due to the limitation of our

GC-analysis system, and thus the results shown in Figure 1 were the combined results of two experiments. The figure indicated the stepwise change in the yields of various products with the reaction temperature and the very stable catalytic activity at the respective reaction temperatures, indicating no deactivation within the present experimental conditions. However, the color of Zn-MFI was changed to light gray from white after the continuous service of 16 h, which indicated the potential deactivation of the catalyst due to a longer reaction time or a higher partial pressure of 2-octanol. The carbon balance was excellent at each temperature, although the product distribution was greatly varied with the temperature. The change in the product distribution will be discussed in the section of reaction pathways. In the current study, most of the experiments were performed in the analysis mode for the C<sub>5</sub>–C<sub>8</sub> compounds (the column set A) because aromatics were the targeted compounds.

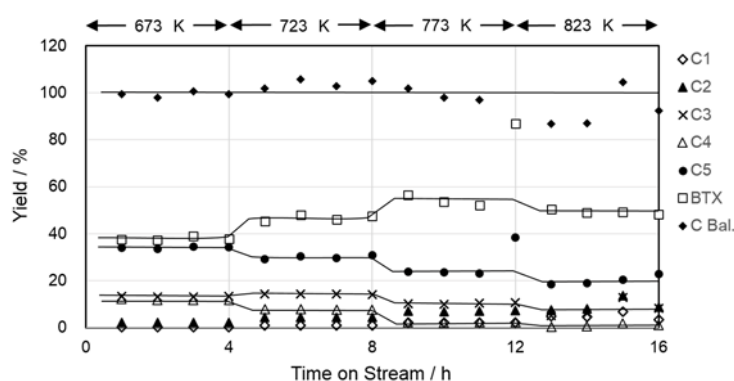


**Figure 1.** Change in the product distribution in the reaction of 2-octanol on Zn-MFI as a function of reaction temperature and time. Reaction conditions: catalyst, Zn-MFI with a silica/alumina ratio 40 and Zn 0.67 wt. %, 0.50 g; total gas flow rate, 20 mL·min<sup>-1</sup> (GHSV 1400 h<sup>-1</sup>); P<sub>2OcOH</sub> 5%; N<sub>2</sub> 95%; 1 atm.

## 2.2. Effects of Zeolite Structure and the Silica Alumina Ratio

The catalytic activity of MFI-, MOR(Mordenite)-, BEA(Beta)-, FAU(Faujasite)-, and LTL(L-type)-containing protons or alkali metal ions is summarized in Figure 2. The extremely low yields of products (a highly undesirable carbon balance) on H-BEA were due to severe coke formation. The product distributions on the zeolites could be classified into three groups: (1) MFI (Benzene 4.6%, Toluene 11.6%, and Xylene 9.3%—A very small amount of ethylbenzene, 0.1%–0.6%, was observed in each experiment, but its amount was not shown unless otherwise stated); (2) MOR (B 0.2, T 0.3, X 0.5), BEA (B 0.5, T 2.1, X 2.6), and H-FAU (B 0.5, T 0.1, X 3.1); and (3) Na-FAU (B 0.0, T 0.9, X 6.9) and K-LTL (B 0.0, T 0.3, X 1.0). The first but not the second and third group of zeolites yielded aromatics as major products. The difference between the second and third groups was the production of 2-octene: thus, the third group of zeolites yielded the dehydrated product of the raw alcohol, which indicated low activity for the scission reaction of carbon-carbon bonds or a milder acidity than those of the first and second group zeolites.

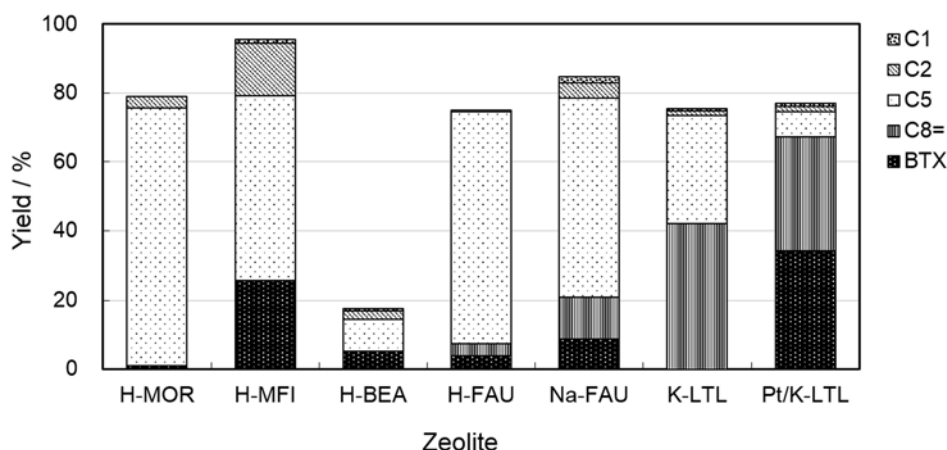


**Figure 2.** Effect of the zeolite structure on the catalytic activity of proton- or alkali ion-exchanged zeolites for reaction of 2-octanol at 773 K. Reaction conditions: catalyst 1.0 g; total gas flow rate  $20 \text{ mL} \cdot \text{min}^{-1}$  (GHSV  $700 \text{ h}^{-1}$ );  $\text{P}_{2\text{o}c\text{OH}}$  5%;  $\text{N}_2$  95%; 1 atm.

The figure indicated that the MFI structure was the most suitable for the production of aromatics among the zeolites employed; thus, MFI was employed hereafter as a parent material for improvement of the catalyst. Importantly, the catalytic activity of K-LTL for aromatization was greatly improved by the addition of platinum as shown in Figure 2, which corresponded to reports that the Pt-K-LTL was active for the aromatization of long-chain hydrocarbons [23–28]. Namely, the dehydration of 2-octanol to 2-octene and the aromatization of the resulting 2-octene were well catalyzed with the acid sites on the LTL zeolite and the loaded Pt, respectively. However, the yield of aromatics was approximately 34%–36% (B 0.0, T 8.1, X 13.9, EB 12.2) at most within the current study and the activity was gradually decreased with the reaction time. These results were inferior to those using Zn-MFI, which will be introduced in the next section, and thus, a detailed investigation on Pt-K-LTL was not performed here.

The catalytic activity of H-MFI was subsequently studied as a function of the silica/alumina ratio. The ratios of the employed MFI zeolites were in the range of 30 to 1880, and the results at 773 K were compared. The yields of aromatics greatly decreased with an increasing ratio; the yields were 34%, 30%, 25%, and 2% at silica/alumina ratios of 30, 40, 90, and 1880, respectively. These results indicated that the number of acid sites on the zeolites was an important factor in controlling the catalytic activity for aromatization due to the widely recognized dependency of the acid-catalyzed reaction on the amount of aluminum ions [14]. The H-MFI zeolite with a silica/alumina ratio of 40 was employed hereafter as the parent zeolite for further experiments because its stability during the catalytic reaction was better than that of H-MFI at a silica/alumina ratio of 30.

### 2.3. Catalysis on Zinc Ion-Exchanged MFI Zeolites

The catalytic activity of various metal ion-exchanged MFI zeolites was examined for the aromatization of 2-octanol, and typical results at 773 K are summarized in Figure 3. The yields of aromatics were in the order of Zn (B 15.3, T 25.8, X 12.3) > Ga (B 12.6, T 23.0, X 10.9) > Ni (B 10.4, T 21.2, X 13.2) > Cu (B 8.3, T 19.2, X 10.3) > Fe (B 7.2, T 15.9, X 10.1) = H (B 7.1, T 14.7, X 9.2). Zinc was selected as the most active component for the targeted reaction. The amount of loaded zinc ions was adjusted at 0.48, 0.67, and 0.88 wt. % using the ion exchange method and at 2.0 and 4.0 wt. % with the conventional

impregnation method. These catalysts provided the yields of aromatics of 62.0 (B 18.6, T 30.2, X 12.5), 63.7 (B 18.8, T 30.6, X 13.8), 63.1 (B 18.3, T 30.1, X 14.3), 62.5 (B 19.3, T 28.8, X 14.3), and 52.6% (B 15.1, T 23.5, X 13.9) at 773 K, indicating little effect of the loading amount on the catalytic activity in the region of 0.5–2.0 wt. %. Moreover, the reaction of 2-octanol proceeded through the decomposition of the reactant to small molecules and the aromatization of the resultant alkanes and alkenes. Several studies reported the similar aromatization reactions of alkanes and alkenes catalyzed by zinc [13,15,17–19] or gallium [14] ion-exchanged MFI zeolites, which were consistent with the present results. The active zinc species were suggested to be  $[\text{Zn}(\text{OH})]^+$  ions [15] or  $[\text{O}^- \text{Zn}^{2+} \text{O}^-]$  species [17], which catalyzed the dehydrogenation of lower alkanes to corresponding alkenes. The little dependence of the catalytic activity on the amount of loaded Zn in the range of 0.5–2.0 wt. % might suggest the former as the active sites. The Zn-MFI zeolite with a silica/alumina ratio of 40 and Zn of 0.67 wt. % prepared by the ion exchange method was employed hereafter as a standard catalyst unless otherwise stated.

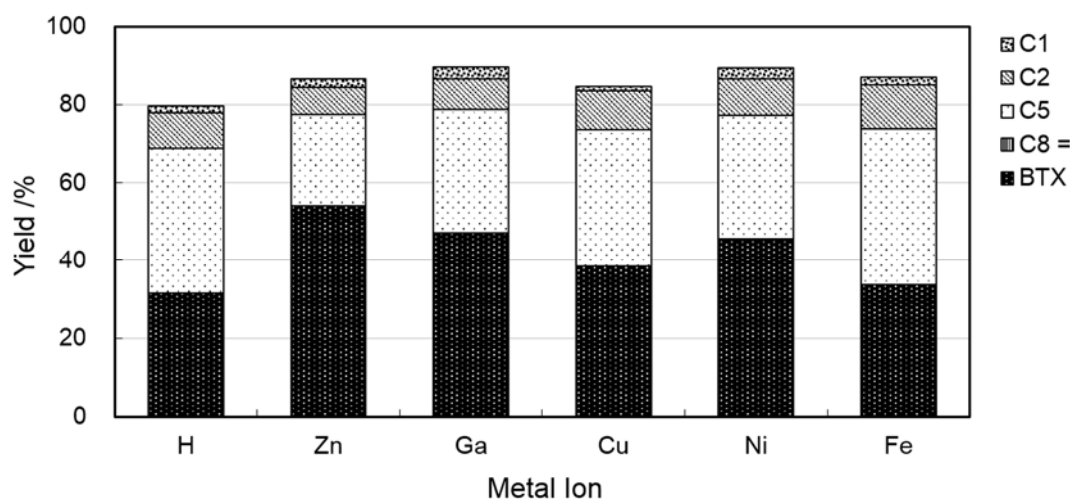


**Figure 3.** Catalytic activity of Zn(0.67 wt. %)-, Ga(0.25)-, Ni(0.24)-, Cu(0.71)-, Fe(0.25)-, and H-MFI zeolites for aromatization of 2-octanol at 773 K. Reaction conditions: catalyst 0.5 g; total gas flow rate  $20 \text{ mL} \cdot \text{min}^{-1}$  (GHSV  $1400 \text{ h}^{-1}$ );  $\text{P}_{2\text{O}_{\text{C}}\text{OH}}$  5%;  $\text{N}_2$  95%; 1 atm.

#### 2.4. Reaction Pathways and Reactivity of Various Compounds

The product distributions on Zn-MFI were investigated as a function of the gas hourly space velocity (GHSV) as shown in Figure 4. The major product at the short contact time (at a high SV) was  $\text{C}_5$  compounds and the yield of aromatics was approximately 30%. The longer contact time decreased the amount of  $\text{C}_5$  compounds and increased the yield of aromatics and hydrogen, which clearly indicated the conversion of  $\text{C}_5$  compounds to aromatics with dehydrogenation. Interestingly, a very small amount of 2-octene was produced in a short contact time, and its amount decreased with increasing contact time, which suggested that 2-octene is an initial intermediate for aromatization. The production of aromatics resulting from the recombination of small hydrocarbons could also be recognized by changes in the amounts of benzene, toluene, and xylene shown in Figure 4B. The amounts of benzene and toluene increased in parallel with the increasing contact time, but those of xylenes showed volcano-shaped dependence on the contact time. These results indicated the major parallel production of BTX and side reactions of xylenes to toluene and/or benzene through demethylation at the longer contact time. Similar

behaviors to those shown in Figure 4 were observed in temperature-dependence (Figure 1). The C<sub>5</sub> and C<sub>3</sub> compounds were produced at lower reaction temperatures and their respective yields indicated stoichiometric decomposition of the C<sub>8</sub> compound. In contrast, aromatics become major at higher temperatures, which accompanies a decrease in the amount of C<sub>2</sub>–C<sub>5</sub> compounds. All of these observations indicated reaction pathways, dehydration of 2-octanol to 2-octene, decomposition of resulting 2-octene to C<sub>5</sub> and C<sub>3</sub> compounds, further decomposition of the C<sub>5</sub> to C<sub>2</sub> and C<sub>3</sub> compounds [14], and, finally, aromatization of C<sub>2</sub> and C<sub>3</sub> compounds with dehydrogenation [15–17,19,20].

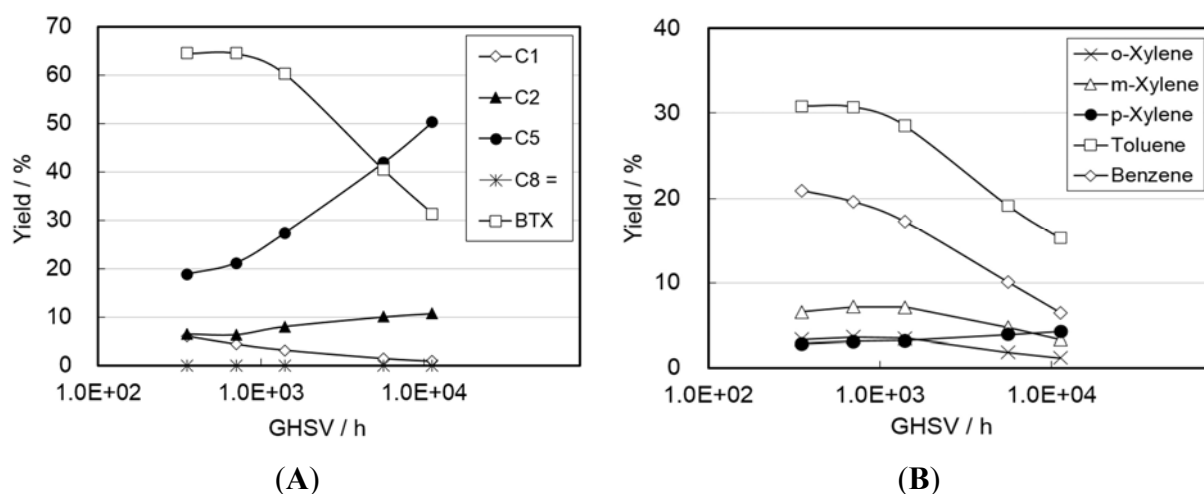


**Figure 4.** Correlation between space velocity and product distribution on Zn-MFI at 773 K. Panels (A,B) summarize the distributions of C<sub>1</sub>–C<sub>8</sub> compounds and aromatics. Reaction conditions: catalyst 0.125–2.00 g; total gas flow rate 20–40 mL·min<sup>-1</sup>; P<sub>2</sub>O<sub>c</sub>OH 5%; N<sub>2</sub> 95%; 1 atm.

These reaction pathways were further supported by the following experiments. Mesoporous silica materials containing very small amounts of aluminum ions, MCM-41, were reported to exhibit weak and uniform acid sites [29–41]. The uniformity of MCM-41 resulted in excellent selectivity of products in various organic synthesis reactions [29–35]. In the current reaction on MCM-41, C<sub>5</sub> and C<sub>3</sub> compounds were obtained stoichiometrically with 100% conversions of 2-octanol at 623–773 K, and no further reaction, such as the scission reaction of C–C bonds of the C<sub>5</sub> compounds, was observed due to the weak acidity of the MCM-41 catalyst [36–41]. The MCM-41 and the Zn-MFI catalysts were mounted in a series into the reactor and used for the reaction of 2-octanol. The product distributions were the same as those shown in Figure 1 within the experimental errors, which supported the previously described reaction mechanism to be correct.

The dependence of the product distribution on the reactants was finally studied to reveal the effect of the functional groups on the reaction pathways. As summarized in Figure 5, C<sub>5</sub>–C<sub>8</sub> alcohols showed very similar product distributions with each other. Little difference of the product distributions indicated that all of the alcohols have the same reaction pathways as that of 2-octanol, that is, the decomposition to C<sub>2</sub>–C<sub>3</sub> hydrocarbons and their recombination to form aromatics. In contrast, the product distributions of the carbonyl compounds were different from those of the corresponding alcohols and dependent on the carbon number of the reactants. With 2-hexanone, the major product among the produced aromatics was benzene. With 2-heptanone and heptanal, it was toluene. In the case of 2-octanone, the amounts of the

produced aromatics were in the order of toluene > benzene > xylene. The carbon number of the major product was not consistent with that of the reactant, but it should be noted that the amount of produced xylene was larger than that from 2-octanol, which suggested the favorable production of xylene from 2-octanone. These consistencies of the carbon numbers of the reactants with those of the products indicated the possibility of direct aromatization of the reactants or long-chain intermediates; that is, the reaction pathways of the carbonyl compounds would be different from those of alcohols.

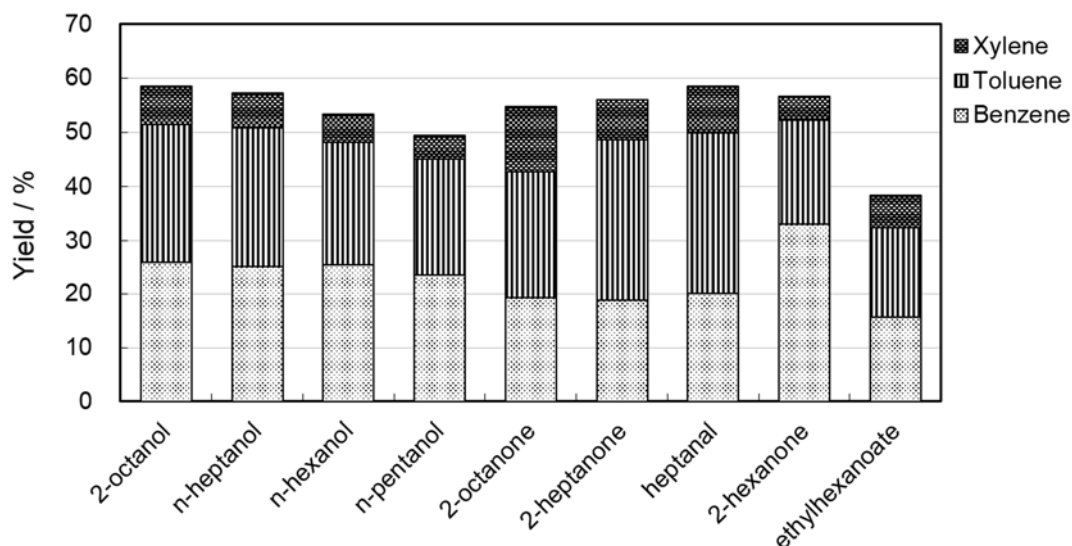


**Figure 5.** Comparison of yields of benzene, toluene, and xylene produced from various oxygenated reactants on Zn-MFI at 773 K. Reaction conditions: catalyst 1.0 g; total gas flow rate  $20 \text{ mL} \cdot \text{min}^{-1}$  (GHSV  $700 \text{ h}^{-1}$ );  $\text{P}_{2\text{O}_5} 5\%$ ;  $\text{N}_2$  95%; 1 atm.

### 3. Experimental Section

#### 3.1. Preparation of Metal Ion-Exchanged Zeolite Catalysts

Metal ion-exchanged zeolite (M-zeolite) catalysts were prepared using a conventional ion exchange method. The properties of the parent zeolites, which were obtained from the Catalysis Society of Japan or purchased from Tosoh Corporation, are summarized in Table 1. The zeolites were ion-exchanged at 353 K for 3 h using aqueous solutions of the metal nitrates Fe, Ni, Cu, Zn, and Ga. After the ion exchange treatments, the samples were washed with deionized water, air-dried at 353 K for 24 h, heated to 823 K in air at a heating rate of 2 K/min, and calcined at the same temperature for 7 h. The amounts of the metal ions loaded were 0.25 (Fe), 0.24 (Ni), 0.71 (Cu), 0.67 (Zn), and Ga (0.25) wt. %, except in the experiments on the dependence of catalytic activity on the exchange level of zinc ions.

**Table 1.** Physico-chemical properties of zeolites used in the present experiments <sup>a</sup>.

Type of Zeolite	SiO <sub>2</sub> /Al <sub>2</sub> O <sub>3</sub> Ratio (mol/mol)	Surface Area (m <sup>2</sup> /g, the BET Method) <sup>b</sup>	Crystal Size (μm)	NH <sub>3</sub> -TPD <sup>c</sup> (mmol/g)
Beta (BEA)	150	560	0.7	0.6
Faujasite (FAU)	5.3	550	0.3	0.7
L-type (LTL)	6	290	0.4	- <sup>d</sup>
ZSM-5 (MFI)	33	330	0.1 × 0.5	1.8
	40	330	2 × 4	1.3
	90	310	2 × 4	0.8
	1880	310	2 × 5	- <sup>d</sup>
Mordenite (MOR)	90	400	0.1 × 0.5	1.2

<sup>a</sup> All data were corrected on the proton-exchanged zeolites; <sup>b</sup> Nitrogen adsorption isotherms at 77 K were used for the calculation of the BET surface areas; <sup>c</sup> Temperature-programmed desorption experiments were carried out to determine amounts of NH<sub>3</sub> adsorbed, the amount of acid sites. The amounts were measured after adsorption of NH<sub>3</sub> at 298 K and subsequent pre-evacuation at 373 K; <sup>d</sup> not determined.

### 3.2. Measurement of Catalytic Activity

The 2-Octanol (>99.5%, Kanto Chemical, Tokyo, Japan) was used without further purification. The continuous flow reactions were performed in a fixed-bed plug-flow reactor made of quartz (i.d. 10 mm) at an atmospheric pressure under the following conditions: catalyst weight 0.05 to 2.0 g (particle diameter, 300–600 μm), total flow rate 12 to 50 mL·min<sup>-1</sup>, partial pressure of 2-octanol (P<sub>2OcOH</sub>) 5% with 95% N<sub>2</sub>. The lengths of the catalyst bed in the reactor were 0.1–4.0 cm and the length of the furnace for heating the reactor was 45 cm, indicating the reaction port isothermal. Prior to the catalytic runs, the catalysts were heated in a N<sub>2</sub> flow at 673 K for 1 h. The crystal sizes of the zeolites employed in this study were 0.1–5 mm as shown in Table 1, indicating that the catalyst performances were measured in diffusion-limiting regime [42].

The products were analyzed with an on-line automatic gas chromatograph (AG-1, Round Science), which was equipped with two sets of three types of packed columns: the first set A, (1) MS 5A; (2) Porapak Q; and (3) Bentone 34 with DIDP (2'-Deoxyinosine 5'-Diphosphoric acid), and the second set B, (1) MS 5A; (2) Porapak Q; and (3') PEG 20 M. The columns 1–2 were independently connected to two TCD detectors to determine the yields of H<sub>2</sub>, N<sub>2</sub>, CO, CO<sub>2</sub>, CH<sub>4</sub>, C<sub>2</sub>H<sub>4</sub>, and C<sub>2</sub>H<sub>6</sub>. The column 3 or 3' was connected to an FID detector to determine the yields of C<sub>5</sub>–C<sub>8</sub> hydrocarbons including aromatics or the yields of C<sub>3</sub>–C<sub>4</sub> hydrocarbons. The switching of the column sets and the measurements, which were obtained twice, were required to determine the entire product distributions of one catalytic run. The present analysis system could not measure the respective amounts of butane, butenes, and butadiene and those of pentane and pentenes; thus, these compounds were expressed as C<sub>4</sub> and C<sub>5</sub> without detailed distinction. The amounts of ethane and ethene or those of propane and propene could be determined separately, but they were also expressed as C<sub>2</sub> or C<sub>3</sub> compounds here because the distinction between alkanes and alkenes did not affect the discussion of the reaction mechanism as shown later. The conversion levels of 2-octanol and yields of hydrocarbon products (C<sub>n</sub>H<sub>x</sub>, n = carbon number) were calculated using Equations (1) and (2), where the partial pressures of 2-octanol before and after the reaction are denoted by P<sub>2OcOH</sub> and P'<sub>2OcOH</sub>, respectively. The amount of N<sub>2</sub> was employed as an internal

standard to determine the conversions. The respective experimental values would have approximately  $\pm 5\%$  of relative errors. The reproducibility of the catalytic performances was very good, as shown in Section 2.3.

$$\text{2-Octanol Conversion (\%)} = 100 (1 - (P'_{2\text{OcOH}}/P_{2\text{OcOH}}) (P_{\text{N}_2}/P'_{\text{N}_2})) \quad (1)$$

$$C_n \text{ Yield (\%)} = 100 (nP'_{C_n}/8P_{2\text{OcOH}}) (P_{\text{N}_2}/P'_{\text{N}_2}) \quad (2)$$

#### 4. Conclusions

The production of aromatics from 2-octanol was investigated on various zeolite catalysts. Zn ion-exchanged MFI zeolites with silica/alumina ratios of 30 to 40 were found to demonstrate high activity for the reaction. The yield of aromatics was approximately 60% at the optimized reaction conditions. The reaction was proposed to proceed via the decomposition of 2-octanol to small alkanes and alkenes and their recombination to form aromatics in the pores of the MFI zeolites. The acid sites would catalyze the dehydration and the scission reaction of C–C bonds, while zinc ions would function in the dehydrogenation of alkanes to alkenes. The aromatization would be catalyzed by both acid sites and zinc ions. It would be worthy to add that 2-octanone, the major impurity (<0.5%) in industrial 2-octanol, gave a similar product distribution to that of 2-octanol and thus would not prevent the present aromatization.

#### Acknowledgments

This work was supported by Grants-in-Aids from Toray Fine Chemicals Co. Ltd., the Japan Society for Promotion of Science (JSPS, METI), and the Advanced Low Carbon Technology Research and Development Program (ALCA, JST).

#### Author Contributions

M.I. conceived and designed the experiments and wrote the paper; R.T. performed the experiments of Sections 2.1–2.3; M.M. performed the experiments of Section 2.4 concerning the reaction mechanism.

#### Conflicts of Interest

The authors declare no conflict of interest.

#### References

1. Castor Oil Production, Extraction, Filtration, Purification&Refining. Available online: <http://www.castoroil.in/extraction/extraction.html> (accessed on 8 December 2015).
2. Carothers, W.H. Synthetic Fiber. U.S. Patent 2130948. 20 September 1938.
3. 2-Octanol. Available online: [http://www.chemicalbook.com/ChemicalProductProperty\\_EN\\_CB3272125.htm](http://www.chemicalbook.com/ChemicalProductProperty_EN_CB3272125.htm) (accessed on 8 December 2015).
4. Caballero, A.; Perez, P.J. Methane as raw material in synthetic chemistry: The final frontier. *Chem. Soc. Rev.* **2013**, *42*, 8809–8820.

5. Bruijninx, P.C.A.; Weckhuysen, B.M. Shale Gas Revolution: An Opportunity for the Production of Biobased Chemicals? *Angew. Chem. Inter. Ed.* **2013**, *52*, 11980–11987.
6. Armor, J.N. Emerging importance of shale gas to both the energy & chemicals landscape. *J. Energy Chem.* **2013**, *22*, 21–26.
7. Chang, C.D. Hydrocarbons from methanol. *Catal. Rev. Sci. Eng.* **1983**, *25*, 1–118.
8. Choudhary, V.R.; Nayak, V.S. Conversion of alcohols to aromatics on H-SM-5: Influence of Si/Al ratio and degree of cation exchange on product distribution. *Zeolites* **1985**, *5*, 325–328.
9. Tynjälä, P.; Pakkanen, T.T.; Mustamäki, S. Modification of ZSM-5 Zeolite with Trimethyl Phosphite. 2. Catalytic Properties in the Conversion of C<sub>1</sub>–C<sub>4</sub> Alcohols. *J. Phys. Chem. B* **1998**, *102*, 5280–5286.
10. Barthos, R.; Széchenyi, A.; Solymosi, F. Decomposition and Aromatization of Ethanol on ZSM-Based Catalysts. *J. Phys. Chem. B* **2006**, *110*, 21816–21825.
11. Tsuchida, T.; Sakuma, S.; Takeguchi, T.; Ueda, W. Direct Synthesis of n-Butanol from Ethanol over Nonstoichiometric Hydroxyapatite. *Ind. Eng. Chem. Res.* **2006**, *45*, 8634–8642.
12. Tsuchida, T.; Yoshikawa, T.; Sakuma, S.; Takeguchi, T.W. Ueda, W. Synthesis of Biogasoline from Ethanol over Hydroxyapatite Catalyst. *Ind. Eng. Chem. Res.* **2008**, *47*, 1443–1452.
13. Mole, T.; Anderson, J.R. The reaction of propane over ZSM-5-H and ZSM-5-Zn zeolite catalysts. *Appl. Catal.* **1985**, *17*, 141–154.
14. Sirokman, G.; Sendoda, Y.; Ono, Y. Conversion of pentane into aromatics over ZSM-5 zeolites. *Zeolites* **1986**, *6*, 299–303.
15. Viswanadham, N.; Pradhan, A.R.; Ray, N.; Vishnoi, S.C.; Shanker, U.; Rao, T.P. Reaction pathways for the aromatization of paraffins in the presence of H-ZSM-5 and Zn/H-ZSM-5. *Appl. Catal. A* **1996**, *137*, 225–233.
16. Bendt, H.; Lietz, G.; Volter, J. Zinc promoted H-ZSM-5 catalysts for conversion of propane to aromatics II. Nature of the active sites and their activation. *Appl. Catal. A* **1996**, *146*, 365–379.
17. Lukyanov, D.B. Application of a kinetic model for investigation of aromatization reactions of light paraffins and olefins over HZSM-5. *Stud. Surf. Sci. Catal.* **1997**, *105*, 1301–1308.
18. Biscardi, J.A.; Meitzner, G.D.; Iglesia, E. Structure and Density of Active Zn Species in Zn/H-ZSM5 Propane Aromatization Catalysts. *J. Catal.* **1998**, *179*, 192–202.
19. Pierella, L.B.; Eimer, G.A.; Anunziata, O.A. Selective ethane conversion into aromatic hydrocarbons over Zn-ZSM-11. *React. Kinet. Catal. Lett.* **1998**, *63*, 271–278.
20. Biscardi, J.A.; Iglesia, E. Reaction Pathways and Rate-Determining Steps in Reactions of Alkanes on H-ZSM5 and Zn/H-ZSM5 Catalysts. *J. Catal.* **1999**, *182*, 117–128.
21. Lusbango, L.M.; Scurrill, M.S. Light Alkanes aromatization to BTX over Zn-ZSM-5 catalysts: Enhancements in BTX selectivity by means of a second transition metal ion. *Appl. Catal. A* **2002**, *235*, 265–272.
22. Miyaji, A.; Sakamoto, Y.; Iwase, Y.; Yashima, T.; Koide, R.; Motokura, K.; Baba, T. Selective production of ethylene and propylene via monomolecular cracking of pentene over proton-exchanged zeolites: Pentene cracking mechanism determined by spatial volume of zeolite cavity. *J. Catal.* **2013**, *302*, 101–114.
23. Bernard, J.R. Hydrocarbons aromatization on platinum alkaline zeolites. In Proceedings of the 5th International Conference on Zeolites, Heyden, London, UK, 2–6 June 1980; pp. 686–693.

24. Besoukhanova, C.; Guidot, J.; Barthomeuf, D.; Breyse, M.; Bernard, J.R. Platinum-zeolite interactions in alkaline L zeolites. Correlations between catalytic activity and platinum state. *J. Chem. Soc. Faraday Trans. 1* **1981**, *77*, 1595–1604.
25. Hughes, T.R.; Jacobson, R.L.; Tamm, P.W. Catalytic processes for octane enhancement by increasing the aromatics content of gasoline. *Stud. Surf. Sci. Catal.* **1988**, *38*, 317–333.
26. Ostgard, D.J.; Kustov, L.; Poepelmeier, K.R.; Sachtler, W.M.H. Comparison of Pt/KL catalysts prepared by ion exchange or incipient wetness impregnation. *J. Catal.* **1992**, *133*, 342–357.
27. Derouane, E.G.; Vanderveken, D. Structural recognition and preorganization in zeolite catalysis: Direct aromatization of *n*-hexane on zeolite L-based catalysts. *Appl. Catal.* **1988**, *45*, L15–L22.
28. Jongpatiwuta, S.; Trakarnroek, S.; Rirksomboon, T.; Osuwan, S.; Resasco, D.E. *n*-Octane aromatization on Pt-containing non-acidic large pore zeolite catalysts. *Catal. Lett.* **2005**, *100*, 7–15.
29. Tanaka, Y.; Sawamura, N.; Iwamoto, M. Highly effective acetalization of aldehydes and ketones with methanol on siliceous mesoporous material. *Tetrahedron Lett.* **1998**, *39*, 9457–9460.
30. Ishitani, H.; Iwamoto, M. Selective aldol reactions of acetals on mesoporous silica catalyst. *Tetrahedron Lett.* **2003**, *44*, 299–301.
31. Iwamoto, M.; Tanaka, Y.; Sawamura, N.; Namba, S. Remarkable Effect of Pore Size on the Catalytic Activity of Mesoporous Silica for the Acetalization of Cyclohexanone with Methanol. *J. Am. Chem. Soc.* **2003**, *125*, 13032–13033.
32. Ishitani, H.; Naito, H.; Iwamoto, M. Friedel-Crafts acylation of anisole with carboxylic anhydrides of large molecular sizes on mesoporous silica catalyst. *Catal. Lett.* **2008**, *120*, 14–18.
33. Murata, H.; Ishitani, H.; Iwamoto, M. Selective synthesis of  $\alpha$ -substituted  $\beta$ -keto esters from aldehydes and diazo esters on mesoporous silica catalysts. *Tetrahedron Lett.* **2008**, *49*, 4788–4791.
34. Murata, H.; Ishitani, H.; Iwamoto, M. Synthesis of Biginelli dihydropyrimidinone derivatives with various Substituents on aluminum-planted mesoporous silica catalyst. *Org. Biomol. Chem.* **2010**, *8*, 1202–1211.
35. Murata, H.; Ishitani, H.; Iwamoto, M. Highly ordered aluminum-planted mesoporous silica as active catalyst for Biginelli reaction and formyl C–H insertion reaction with diazo ester. *Phys. Chem. Chem. Phys.* **2010**, *12*, 14452–14455.
36. Iwamoto, M.; Kosugi, Y. Highly Selective Conversion of Ethene to Propene and Butenes on Nickel Ion-Loaded Mesoporous Silica Catalysts. *J. Phys. Chem. C* **2007**, *111*, 13–15.
37. Ikeda, K.; Kawamura, Y.; Yamamoto, T.; Iwamoto, M. Effectiveness of the template-ion exchange method for appearance of catalytic activity of Ni-MCM-41 for the ethene to propene reaction. *Catal. Commun.* **2008**, *9*, 106–110.
38. Haishi, T.; Kasai, K.; Iwamoto, M. Fast and Quantitative Dehydration of Lower Alcohols to Corresponding Olefins on Mesoporous Silica Catalyst. *Chem. Lett.* **2011**, *40*, 624–626.
39. Iwamoto, M.; Kasai, K.; Haishi, T. Conversion of Ethanol into Polyolefin Building Blocks: Reaction Pathways on Nickel Ion-loaded Mesoporous Silica. *ChemSusChem* **2011**, *4*, 1055–1058.
40. Mizuno, S.; Kurosawa, M.; Tanaka, M.; Iwamoto, M. One-path and Selective Conversion of Ethanol to Propene on Scandium-modified Indium Oxide Catalysts. *Chem. Lett.* **2012**, *41*, 892–894.
41. Iwamoto, M.; Mizuno, S.; Tanaka, M. Direct and Selective Production of Propene from Bio-Ethanol on Sc-Loaded In<sub>2</sub>O<sub>3</sub> Catalysts. *Chem. Eur. J.* **2013**, *19*, 7214–7220.

42. Nakasaka, Y.; Okamura, T.; Konno, H.; Tago, T.; Masuda, T. Crystal Size of MFI-type Zeolite for Catalytic Cracking of *n*-Hexane under Reaction-control Condition. *Microporous Mesoporous Mater.* **2013**, *182*, 244–249.

© 2015 by the authors; licensee MDPI, Basel, Switzerland. This article is an open access article distributed under the terms and conditions of the Creative Commons Attribution license (<http://creativecommons.org/licenses/by/4.0/>).